

AFOSR 60-65

THE UNIVERSITY OF MICHIGAN  
COLLEGE OF ENGINEERING  
Department of Aeronautical and Astronautical Engineering

Final Report

STAGNATION POINT FLUCTUATIONS ON BODIES OF REVOLUTION WITH HEMISPHERICAL NOSES

A. M. Kuethe  
W. W. Willmarth  
G. H. Crocker

ORA Project 02753

under contract with:

AIR FORCE OFFICE OF SCIENTIFIC RESEARCH  
AIR RESEARCH AND DEVELOPMENT COMMAND  
CONTRACT NO. AF 49(638)-336  
WASHINGTON, D.C.

administered through:

OFFICE OF RESEARCH ADMINISTRATION      ANN ARBOR

June 1960



TABLE OF CONTENTS

SUMMARY .....	3
ACKNOWLEDGEMENT.....	4
INTRODUCTION .....	5
EQUIPMENT .....	6
RESULTS .....	7
Pressure Distribution .....	7
Turbulence Contours .....	8
Turbulence near Surface at $\phi = 7^\circ$ .....	8
Effects of Model Mounting and of Flow over Afterbody ....	9
DISCUSSION .....	12
RESULTS .....	15
REFERENCES .....	17
TABLES 1-3 .....	18-20
FIGURES 1-8.....	21-26



## SUMMARY

The turbulent fields outside of the boundary layer near the noses of axially symmetric bodies with hemispherical noses have been studied by means of the hot-wire anemometer. Measurements in a low turbulence wind tunnel over a range of Reynolds numbers show that the rms streamwise fluctuations in the nose region are larger than in the free stream. Large negative spatial correlation factors between streamwise fluctuations at  $\pm 7^\circ$  from the axis at low speeds and in a supersonic tunnel at Mach 2.45 indicate that the fluctuations in the nose region are coupled with a random motion of the stagnation point. The normalized energy spectra of the fluctuations at  $7^\circ$  are found to scale with the free stream wave number  $n/U_\infty$ , where  $n$  is the frequency of the fluctuations, over a ten-fold range in model diameter and a forty-fold range in Reynolds number. These normalized spectra also show a shift toward lower frequencies compared with free stream turbulence. Possible connection between these phenomena and heat transfer measurements from bodies as affected by turbulence are pointed out.

#### ACKNOWLEDGEMENT

Most of the experimental work reported here was supported by the USAF Office of Scientific Research under Contract No. AF 49(638)-336. A few of the measurements and most of the analysis were supported by the US Air Force Research Division, Aeronautical Research Laboratories, under contracts AF 33(616)-6856 and AF 33(616)-7628. Most of the results given are also reported in the PhD Thesis of the third author.<sup>1</sup>

The authors are indebted to C. E. Wooldridge, Ralph Deitrick, and Norman Hawk for some of the experimental results.

## INTRODUCTION

Several investigators<sup>2,3,4,5</sup> have reported anomalous effects of stream turbulence on the measured heat transfer near the forward stagnation point of blunt two-dimensional bodies. The integrated heat transfer rates, as well as the local values throughout the region of laminar boundary layer, showed large increases when the turbulence level in the stream was increased, even when the Reynolds number was well below the critical value for the rearward motion of the flow separation point.

A connection has been conjectured<sup>5</sup> between these measurements and the relatively high turbulence level near the stagnation point of a blunt two-dimensional body, as discovered by Piercy and Richardson<sup>6</sup>. They found in a wind tunnel of high turbulence level that the amplitude of the fluctuations near the nose of a streamlined strut reached a value about 4.5 times that in the free stream, and that the region of increased turbulence extended about  $1/4$  chord ahead of the body.

A detailed study of the boundary layer near the nose of blunt bodies of revolution, particularly with regard to transition at hypersonic speeds, is being undertaken at The University of Michigan. During the course of the preliminary low speed phase of the investigation, it was observed that velocity fluctuations greater in magnitude than those in the main stream occurred near the stagnation point.

Accordingly, the fluctuation field in the vicinity of the nose was studied in some detail. While the measurements of Piercy and Richardson<sup>6</sup> concerned two-dimensional bodies, the measurements reported here represent features of the three-dimensional counterpart of the fluctuation field they observed.

## EQUIPMENT

The experimental results were obtained in the 5 x 7 feet low-turbulence tunnel and in the 8 x 13 inch supersonic tunnel at the University of Michigan.

The low-turbulence tunnel is of the closed return type with dimensions shown in Fig. 1. The air speed range is 0-270 ft/sec.

The supersonic tunnel is of the intermittent blow-down type; dry air at atmospheric pressure, stored in a collapsible container, discharges through the test section into manifolded evacuated tanks. The Mach number range is 1.4 to 5 with a maximum run duration of about 20 seconds. The measurements described here were made at a Mach number of 2.44.

Three axially-symmetric bodies, shown in Fig. 2, were used for the subsonic tests. They have hemispherical noses with diameters 20, 11.7, and 2 inches and fineness ratios 5.2, 6.3, and 17, respectively. The nose of the 20 inch model is of aluminum, the 11.7 inch is of wood and the 2 inch is of plastic. The afterbodies were fabricated of sheet metal and wood with steel re-enforcing. For the 20 inch model a heating coil was installed so that the forward  $10^{\circ}$  could be heated to a few hundred degrees above room temperature.

The supersonic measurements were made with the same 2 inch sphere which had been faired for the subsonic measurements. The sphere was mounted on a sting 0.875 inches in diameter.

A Shapiro and Edwards model 50 four channel hot-wire anemometer system was used throughout the program for measurements of the mean and



fluctuating velocities. The amplifier has nearly constant amplification in the range 1 to 20,000 cps.

A low-frequency wave analyzer with frequency range 1.6 to 160 cps, developed by M. S. Uberoi at the University of Michigan, was used for spectrum analysis of the hot-wire signal. For a few of the measurements the equipment was modified to reduce the frequency range by a factor of 10.

The hot-wires used had diameters of 0.0002 to 0.0004 inches and lengths 0.015 to 0.03 inches. Platinum wires were used during the early tests, but because of their short life at the higher subsonic and at the supersonic speeds, tungsten wires were used in the later phases.

Measurements of the turbulence in the nose region were made for the most part by means of a traversing unit shown in Fig. 3. The position of the wire could be adjusted in the radial, meridional, and azimuthal direction. The motion of the wire in the azimuthal direction was limited to about one inch, that in the meridional direction from near  $0^\circ$  to  $63^\circ$ , and that in the radial direction was  $\pm 0.05$  inches about a pre-set position.

## RESULTS

Pressure Distribution. The pressure distribution was measured in the nose region of the 20" body and compared with that for an inviscid incompressible flow. The plot of the pressure coefficient is shown in Fig. 4.

Turbulence Contours. Contours of constant  $u'_s/u'_\infty$ , the ratio of the rms streamwise velocity fluctuations in the nose region of the 20" diameter body to that in the free stream, are shown in Fig. 5 for two Reynolds numbers.

Relatively high fluctuation levels were measured within  $1^\circ$  of the model axis ahead of the stagnation point. These higher levels close to the axis are believed to have been caused by interference from the probe support. This conclusion is based on the sudden violent change in signal from a supplemental hot-wire located near the model surface at  $\phi = -7^\circ$  when the primary survey hot-wire was brought within  $+1^\circ$  of the model axis. The validity of the data near the axis is therefore considered doubtful and the turbulence contours in this region are shown as dashed lines in Fig. 5.

Turbulence near Surface at  $\phi = 7^\circ$ . Measured values of  $u'_s/U_\infty$ , the relative rms streamwise fluctuations, the surface of the three bodies at  $\phi = 7^\circ$  are shown in Fig. 6\*. The positions of the hot-wires in terms of radius of the body and boundary layer thickness are shown in Table 1.

The normalized energy spectra of the fluctuations at the positions designated in Table 1 and in the free stream are shown in Fig. 7. These were measured by the harmonic analyzer and used a constant bandwidth of 0.8 cps. The spectra at extremely low frequencies were measured with a much narrower band width but were corrected to 0.8 cps

---

\*These data and some of the spectrum and spatial correlation data given in the following paragraphs have been previously reported in reference 7.

bandwidth. The individual distributions were normalized so that

$$\int_0^{\infty} j \, d(n/U_{\infty}) = 1 \text{ ft.}^{-1}$$

where the relative energy in a given frequency band per unit  $n/U_{\infty}$  is  $j u'_s{}^2/U_{\infty}{}^2$ , with  $u'_s{}^2/U_{\infty}{}^2$  given by Fig. 6.

These spectrum measurements were supplemented by measurements of the spatial correlation factors between the speed fluctuations at  $\phi = \pm 7^\circ$  with both wires at the radial positions given in Table 1. The results are shown in Table 2 where

$$R = \overline{u_1 u_2} / u_1' u_2'$$

is the correlation factor. The subscripts refer to the responses of the respective wires. Most of the measurements were made with the frequency band  $0.3 < n < 20,000$  cps, but for a few of them the upper cut-off was changed to 10, 100, or 1000 cps.

In addition to the subsonic tests, measurements of the correlation factor were made on the 2" sphere at Mach 2.44 in the supersonic tunnel. When the hot-wire response over the range 10 to 20,000 cps was used, the correlation was near zero. However, when those components with frequencies above 50 cps were suppressed, the correlation factor was -0.4. This result is entered in Table 2.

Effects of Model Mounting and of Flow over Afterbody. To determine if the high velocity fluctuation levels at the nose were influenced by the hot-wire support or by the model after-body configuration, a number of changes were made sequentially. Alternate hot-wire supports with widely different interference to the flow over the body

gave no significant change in the fluctuation level. For purposes of reference, the  $7^{\circ}$  station on the 20-inch diameter model (see Table 1) was used for all speed conditions. Fluctuation levels and spectral energy densities of the velocity were measured at this point as changes were made to the model and its support system.

With the model mounting struts attached directly to the wood floor of the tunnel test section, a coupling between the tunnel and the model was first considered a likely cause of the high fluctuation levels near the nose. Therefore, the model mounting system was radically changed. A structure of steel 6" x 6" I-beams was fabricated to serve as the support for the model mounting struts. This I-beam structure was placed beneath the tunnel test section and supported on wood pads laid on the concrete floor of the wind tunnel building. This floor serves as the building foundation and is isolated from the tunnel structure. The streamlined model mounting struts passed from the support structure through holes in the test section floor to the model. The clearance between the struts and the floor was sealed with rubber sheeting.

Additional support was provided the tip of the model tail cone by three cables, one secured to the concrete floor and the other two to the steel beam structure of the wind tunnel building through shock cord links. These cables passed through holes in the test section walls without contact to form a "Y" support structure in a plane normal to the flow direction.

Test runs of the velocity fluctuations at the reference position with the new model mount gave velocity fluctuation levels essentially the same as those with the initial mounting system.

The possibility was next investigated that these fluctuations might be the result of aerodynamic feed-back from turbulent flow over the surface and in the wake of the model to the flow near the nose.

To determine whether the unsteadiness could be caused by unsteadiness of the laminar separation point near  $\phi = 80^\circ$ , fluctuations with the model in the "clean" configuration were compared with those utilizing a boundary layer trip wire extending peripherally around the nose surface at an angle  $\phi$  of  $60^\circ$ . Velocity fluctuations were not significantly affected.

The possibility that fluctuations at the nose were being transmitted through the potential flow from the aft region of the model was explored with a major change to the model configuration. An annular metal shroud with a 12-inch chord and no camber was mounted with its trailing edge 3 inches ahead of the tip of the tail cone (see Fig. 4). Velocity fluctuations at the nose reference position were then measured with the shroud open and also with its annular opening completely closed. The latter configuration gave a bluff body type of wake visually shown by the violent action of wool tufts located on the rear part of the tail cone and the outside surface of the shroud. The effect these configuration changes had on the fluctuation level at the reference position was not significant.

Table 3 summarizes the velocity fluctuation levels for these changes in configuration. The variations in data for all configurations and velocities are within the range of reproducibility of the fluctuation level data.

The spectral energy distribution of the velocity fluctuations was also measured for the various configurations at three nominal free-

stream velocities -- 50, 100 and 200 ft/sec. The results, shown in Fig. 8, show close similarity between the spectral distributions for the "clean" model, for the model with boundary layer trip and for the model with the different shroud configurations.

## DISCUSSION

The first question to be answered with regard to the velocity fluctuations in the nose region of a body is: To what extent is their origin associated with the model mounting, with unsteadiness of the boundary layer transition point, or with the unsteady wake? The data given in Table 3 and in Fig. 8 demonstrate that the effects of these influences are within the experimental scatter of the hot-wire measurements. We therefore conclude that the characteristics of the turbulence field described by Figs. 5, 6, and 7 and Table 2 depend on the turbulence in the main flow, as influenced by Reynolds number and the nose shape.

Comparison of results given in Fig. 5 for two Reynolds numbers shows that the region in which the turbulence exceeds the free stream value extends considerably farther out from the body for the lower Reynolds number than for the higher.

It is interesting to interpret these regions of relatively high turbulence in terms of boundary layer thicknesses. The calculated boundary layer thicknesses, given by  $\delta/R = 2.26 \sqrt{\nu/U_\infty \rho}$  (almost constant over the range  $0 < \phi < 25^\circ$ ) are 0.0022 and 0.00155, respectively, for the lower and higher Reynolds numbers. The magnitude of the turbulence exceeds the free stream value in the layer out to about

$y/R = .04$  at  $\phi = 7^\circ$  at both Reynolds numbers. Thus, at  $\phi = 7^\circ$  the region of excess turbulence extends to  $18\delta$  and  $26\delta$ , respectively, at the lower and higher Reynolds numbers. At  $\phi = 20^\circ$  the region of excess turbulence extends to  $55\delta$  ( $y/R = 0.12$ ) and  $40\delta$  ( $y/R = .06$ ), respectively, at the lower and higher Reynolds numbers. This latter comparison is probably significant, but at the  $7^\circ$  position the contours are so close together that the difference between  $18\delta$  and  $26\delta$  is probably within the experimental error.

The data in Figs. 5 and 6 indicate that the amplitudes of low frequency components near the stagnation point are considerably higher than in the free stream turbulence. Further, the correlation factors given in Table 2 show that the major portion of the turbulent energy at  $\phi = 7^\circ$  is identified with a random motion of the stagnation point. Peterson and Horton<sup>10</sup> also identified random motion of the stagnation point on the basis of pressure measurements at the nose.

The coupling of the fluctuations with the motion of the stagnation point was further demonstrated by another observation. When a cruciform arrangement of two perpendicular plates was fitted to the nose, thus fixing the stagnation point, the fluctuations at the  $7^\circ$  position fell to a very low value. However, when new nose shapes, pointed or rounded, were fitted to the region  $-2 < \phi < 2^\circ$ , the magnitude of the fluctuations at the  $7^\circ$  position was not substantially altered.

The data of Fig. 6 show that the rms value of the streamwise fluctuation at  $\phi = 7^\circ$  is a function of the velocity and of model size. The fact that the magnitude of  $u'_s$  is greater than  $u'_\infty$  for all of the measurements is not significant because the lateral components in the free stream,  $v'_\infty$  and  $w'_\infty$  are each about twice  $u'_\infty$  and, further, near

the nose there is a good possibility that energy transferred from  $v'_{\infty}$  and  $w'_{\infty}$  accounts for part of  $u'_s$ . For instance, a lateral component, if its scale is large enough, in effect tilts the incident airstream establishing a new stagnation point and thus changing its location relative to the hot wire; in this way energy is transferred from  $v'_{\infty}$  or  $w'_{\infty}$  to  $u'_s$ .

The inverse relationship between model size and  $u'_s$  shown in Fig. 6 agrees with that expected, since small scale turbulence will influence the flow over small diameter bodies to a greater extent than over large. In other words the flow field over a body of given diameter would be insensitive to small scale eddies in the incident flow but would approach that corresponding to a change in  $U_{\infty}$  for large scale eddies. We find, for instance, that the data given in Fig. 6 can be expressed by the relation

$$\frac{u'_s}{u'_{\infty}} D^{\frac{1}{4}} = 1.85 \text{ (ins)}^{\frac{1}{4}}$$

with an rms deviation of 4.5%. The scale of the free stream turbulence as shown by the spectra of Fig. 7, is independent of wind speed, and so does not occur in the above expression. More observations with different magnitudes and scales of free stream turbulence will be necessary to identify a quantitative description of the relationship.

The spectra of Fig. 7 indicate two interesting features. First, the normalized spectra near the nose scale with  $n/U_{\infty}$  ( $n$  is the frequency in cps), that is, with free stream wave number, independent of Reynolds number and relative scale of the turbulence. Second, the



observations near the nose at a given  $U_\infty$  show a higher relative concentration of energy at low frequencies, compared with the free stream turbulence. The existence of this spectrum shift is consistent with the rationalization given above for the variation of the rms fluctuations with relative scale.

The correlation factor of  $-0.4$  at  $\pm 7^\circ$  on the 2" sphere at Mach number 2.44 (Table 2) was measured only after all frequencies above 50 cps were suppressed. This result indicates the presence in the supersonic airstream of relatively high frequency, positively correlated fluctuations, probably pressure waves. The negative correlation indicates that at supersonic as well as at subsonic speeds a random low frequency motion of the stagnation point occurs.

This stagnation point motion could be expected to influence the average heat transfer near the stagnation point. As was pointed out in the Introduction, measurements in several laboratories show that the local heat transfer rate to blunt bodies in supersonic flow reaches a maximum value a short distance from the stagnation point of the main flow<sup>8</sup>. It is to be expected that the rate would be nearly constant on the portion of the surface covering the excursions of the stagnation point, though why it should reach a maximum off the axis is unclear.

## RESULTS

1. The turbulent field outside of the boundary layer near the nose of a blunt body in a low turbulence incompressible flow exhibits the following characteristics.

- a) The rms streamwise velocity fluctuations in the nose region are larger than those in the free stream. The region in which the ratio of the two rms values exceeds unity extends

many boundary layer thicknesses out from the body.

The region extends farther out at  $Re = 10^6$ . However, the fact that a Reynolds number based on the scale of the turbulence is different for the two sets of observations prevents a quantitative conclusion.

b) Large negative spatial correlation factors at  $\phi = \pm 7^\circ$  indicate that the velocity fluctuations near the stagnation point are closely coupled with a random motion of the stagnation point.

c) The expression  $D^{\frac{1}{4}} u'_s / u'_\infty = 1.85$ , with an rms deviation of 4.5%, describes all of the observations. This result agrees qualitatively with the expectation that when the larger scale turbulence elements in the free stream pass over the body, their effect on the flow will be greater than for the smaller scale elements.

d) The normalized energy spectra at  $\phi = 7^\circ$  scale with the free stream wave number. The observations cover a forty-fold range in Reynolds number and a ten-fold range in body diameter.

e) The normalized spectra of the fluctuations at  $7^\circ$  indicate a shift toward lower frequencies, compared with the free stream turbulence at the same  $U_\infty$ . This shift is in qualitative agreement with the rationalization given under c.

2. A spatial correlation factor of -0.4 at  $\phi = \pm 7^\circ$  on a sphere in a Mach 2.44 flow indicates a random relatively low frequency motion of the stagnation point similar to that found at low speeds.

## REFERENCES

1. a) Gage H. Crocker, "Stagnation Point Fluctuations and Boundary Layer Stability on Bodies of Revolution with Hemispherical Noses," PhD Thesis, The University of Michigan. See also b) A. M. Kuethe, W. W. Willmarth, and Gage H. Crocker, "Turbulence Field Near the Stagnation Points on Blunt Bodies of Revolution," Proceedings of the Heat Transfer and Fluid Mechanics Institute, University of Southern California, June 1961.
2. W. H. Giedt, "Effect of Turbulence Level of Incident Airstream on Local Heat Transfer and Skin Friction on a Cylinder," Jour. Aero. Sciences, Vol. 18, 1951, pp. 725-730, 776.
3. J. Kestin and P. Maeder, "Influence of Turbulence on Transfer of Heat from Cylinders," NACA TN 4018, 1957.
4. R. A. Seban, "The Influence of Free Stream Turbulence on the Local Heat Transfer from Cylinders," Trans. ASME, Jour. Heat Transfer, Vol. 82, 1960, pp. 101-107.
5. H. Shuh, "A New Method for Calculating Laminar Heat Transfer on Cylinders of Arbitrary Cross-Section and on Bodies of Revolution at Constant Variable Wall Temperature," Kungl Tekniska Hogskolan Technical Note No. 33, Stockholm, June, 1953.
6. Piercy, N. A. V. and Richardson, E. G., "The Variation of Velocity Amplitude Close to the Surface of a Cylinder Moving Through a Viscous Fluid," Phil. Mag., Vol. 6, 1928.
7. A. M. Kuethe, W. W. Willmarth, and G. H. Crocker, "Stagnation Point Fluctuations on a Body of Revolution," Physics of Fluids, Vol. 2, No. 6, pp. 714-716, Nov.-Dec., 1959.
8. S. M. Hastings and A.J. Chones, "Supersonic Aerodynamic Heating of a Yawed Sphere-Cone Wind Tunnel Model," NAVORD Report 6812, June 1960.
9. H. Schlichting, "Boundary Layer Theory," McGraw-Hill Book Co., 1955.
10. J. B. Peterson, and E. S. Horton, "An Investigation of the Effect of a Highly Favorable Pressure Gradient on Boundary Layer Transition as Caused by Various Types of Roughness on a 10 ft. Diameter Hemisphere at Subsonic Speeds," NASA Memo 2-8-596, 1959.

TABLE 1

HOT WIRE POSITIONS FOR  
VELOCITY FLUCTUATION MEASUREMENTS

MODEL DIAMETER	$\phi$	y	y/R	$U_{\infty}$	$\delta$ (theory)	y/ $\delta$	$R_e = \frac{U_{\infty} D}{\nu}$
INCHES	DEGREES	INCHES	----	Ft/Sec	INCHES	---	x $10^{-5}$
2.0	7°	.034	.034	50	.0100	3.4	.52
				100	.0071	4.8	1.0
				200	.0050	6.8	2.1
11.7	7°	.10	.017	50	.024	4.2	3.1
				100	.017	5.9	6.1
				200	.012	8.3	12.2
20.0	7°	.17	.017	50	.031	5.4	5.2
				100	.022	7.6	10.4
				200	.016	10.7	20.9

TABLE 2

VELOCITY CORRELATION FACTORS FOR  $\phi = \pm 7^\circ$  FROM NOSE

<u>D</u> <u>ins.</u>	<u>U</u> <u>ft/sec</u>	<u>R(u<sub>1</sub>,u<sub>2</sub>)</u>	<u>Band Pass</u> <u>cps &lt; n &lt; cps</u>
2.0	125	- .91	1 < n < 20,000
	125	- .94	10 < n < 20,000
	125	- .90	100 < n < 20,000
	125	small but negative	1,000 < n < 5,000
	M = 2.44	small but positive	10 < n < 20,000
11.7	48.4	- .40	1 < n < 50
	94.4	- .77	1 < n < 20,000
	94.4	- .84	1 < n < 20,000
	198	- .65	1 < n < 20,000
20	49	- .79	1 < n < 20,000
	98	- .65	1 < n < 20,000
	206	- .72	1 < n < 20,000
	173	- .75	100 < n < 20,000

TABLE 3

EFFECT OF CHANGES IN MODEL CONFIGURATION ON THE VELOCITY  
FLUCTUATION LEVEL,  $u'_s / U$  NEAR THE NOSE OF A 20-INCH DIAMETER  
HEMISPHERICAL NOSED MODEL AT  $\phi = 7^\circ$ ,  $y = 0.17''$ .

NOMINAL FREE STREAM VELOCITY

MODEL CONFIGURATION	<u>50 FPS</u>	<u>100 FPS</u>	<u>200 FPS</u>
	$u'_s / U$ %	$u'_s / U$ %	$u'_s / U$ %
CLEAN	.033	.059	.092
	.033	.062	.100
	.037	.064	.110
	.042		
.073-INCH TRIP WIRE at $\phi = 60^\circ$	----	.051	.102
12-INCH CHORD SHROUD OPEN	.037	.066	.110
	.038		
12-INCH CHORD SHROUD BLOCKED	.038	.061	.105

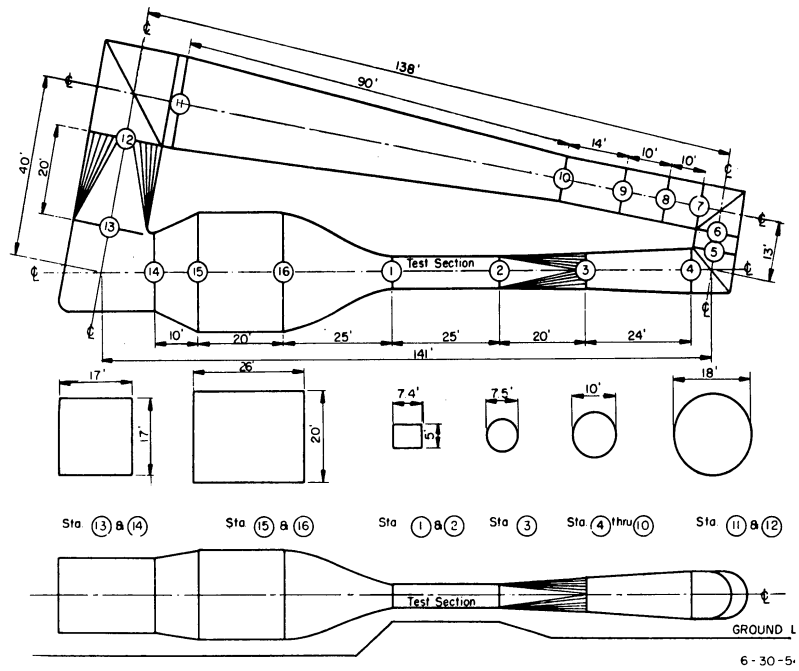


Fig. 1. Drawing of the Low Turbulence Wind Tunnel at the University of Michigan. Six screens are located between stations 14 and 16.

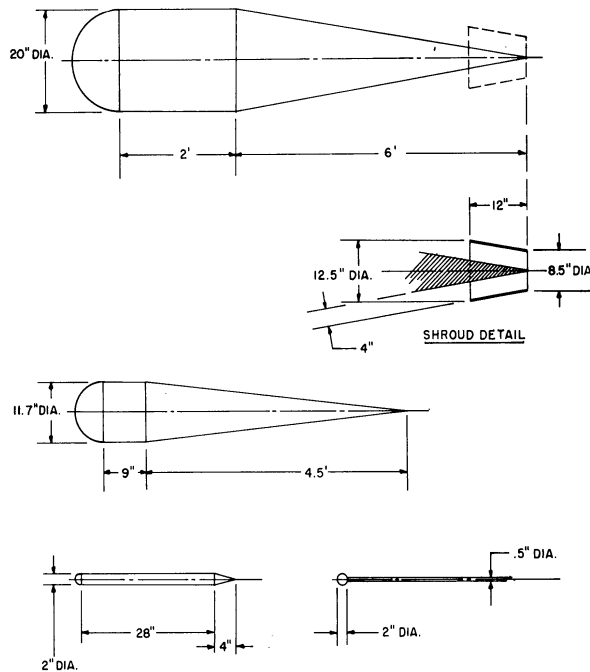


Fig. 2. Bodies of Revolution used in the Investigation. Details of the shroud used in attempt to eliminate or intensify movement of the stagnation point. Model at lower right was used in supersonic test.

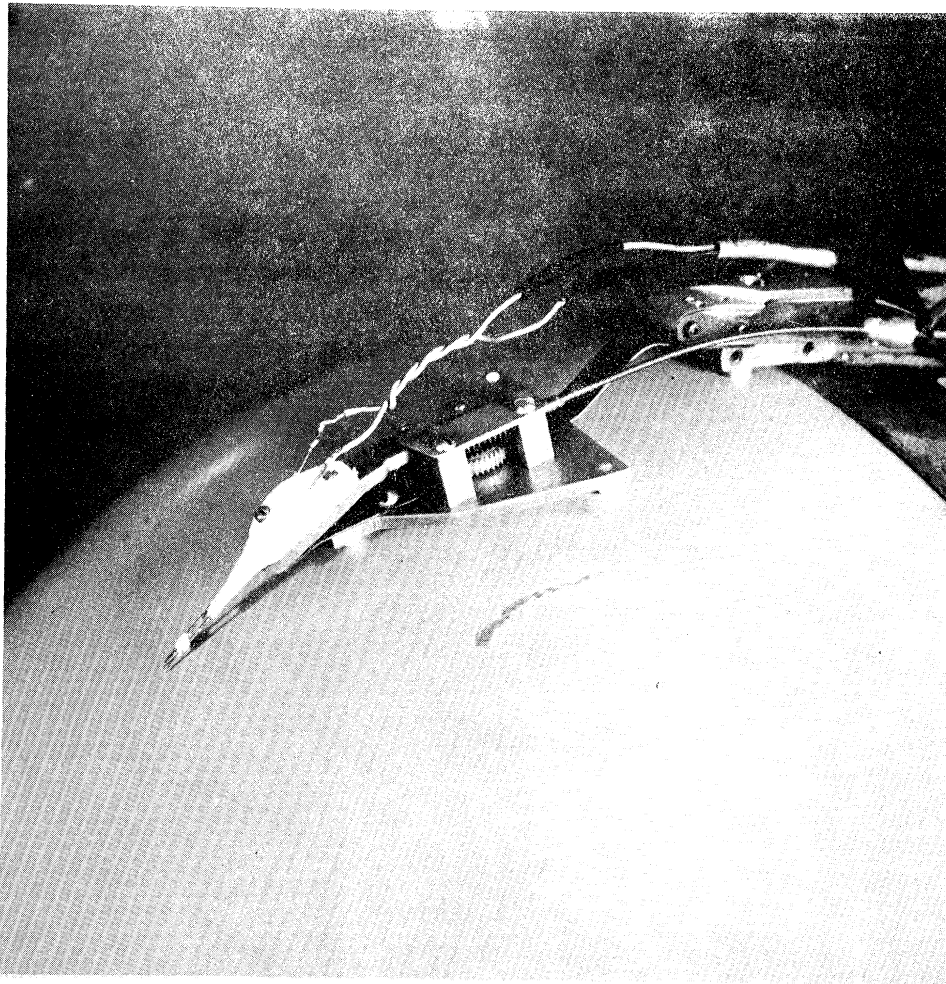


Fig. 3. Photograph of the hot-wire traverse head

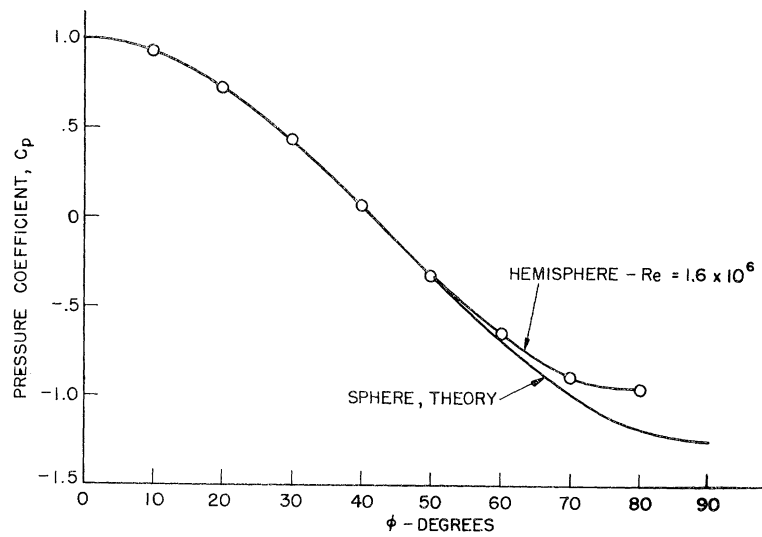


Fig. 4. Pressure distribution over nose of 20" diameter body



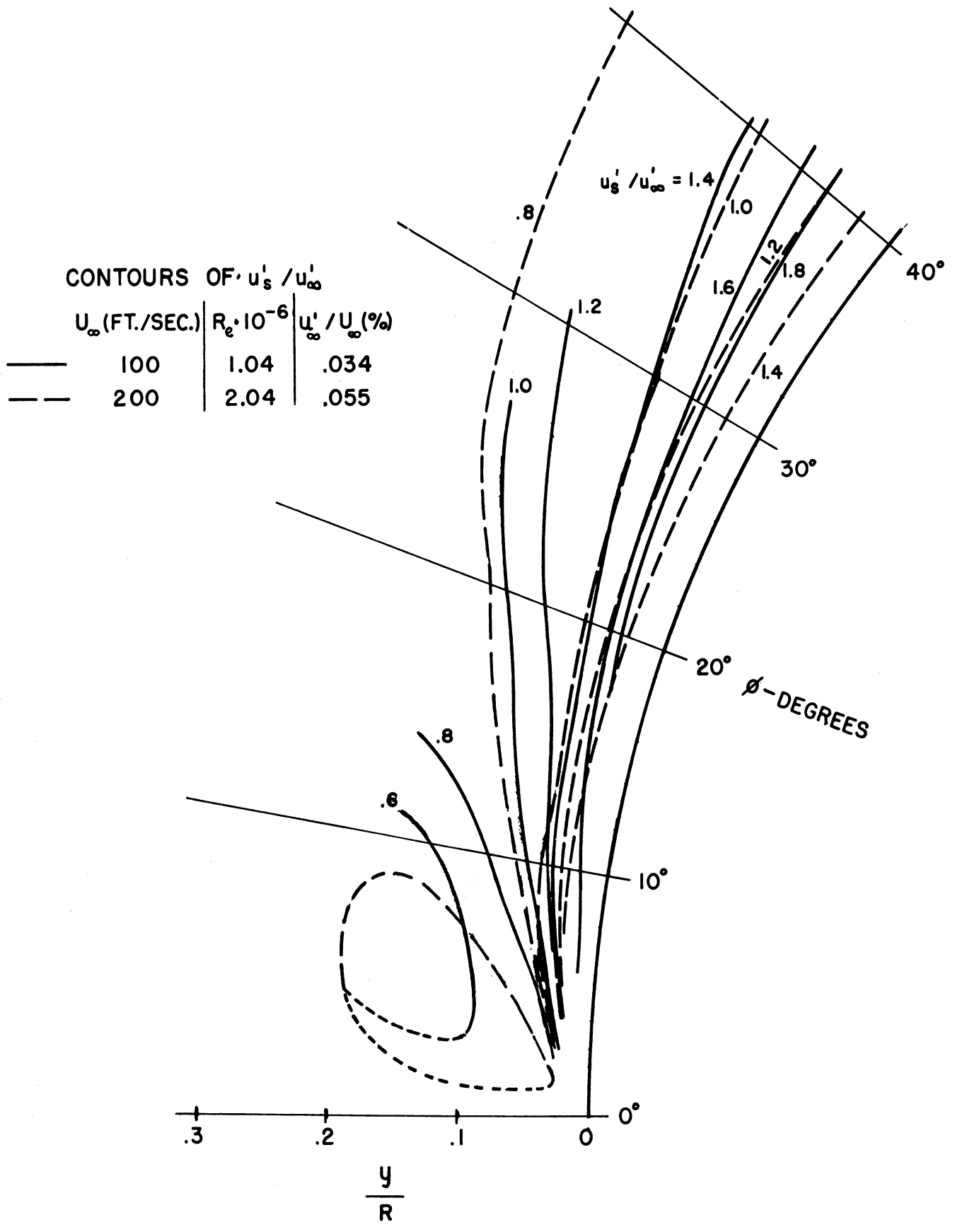


Fig. 5. Contours of equal ratio of local streamwise fluctuation in the nose region of the 20 in. diameter body.

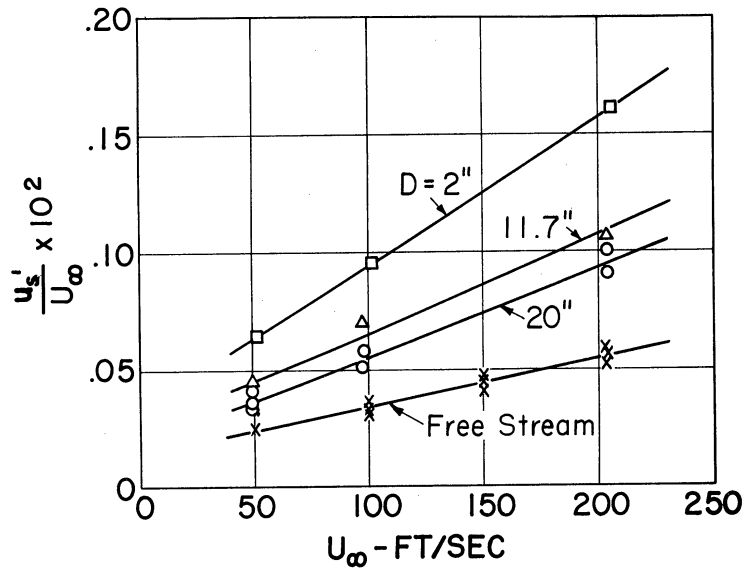


Fig. 6. Root-mean-square streamwise fluctuations at  $7^\circ$  from nose outside of boundary layer as function of body diameter and air speed. See Table 1 for distance of hot-wire from body surface.

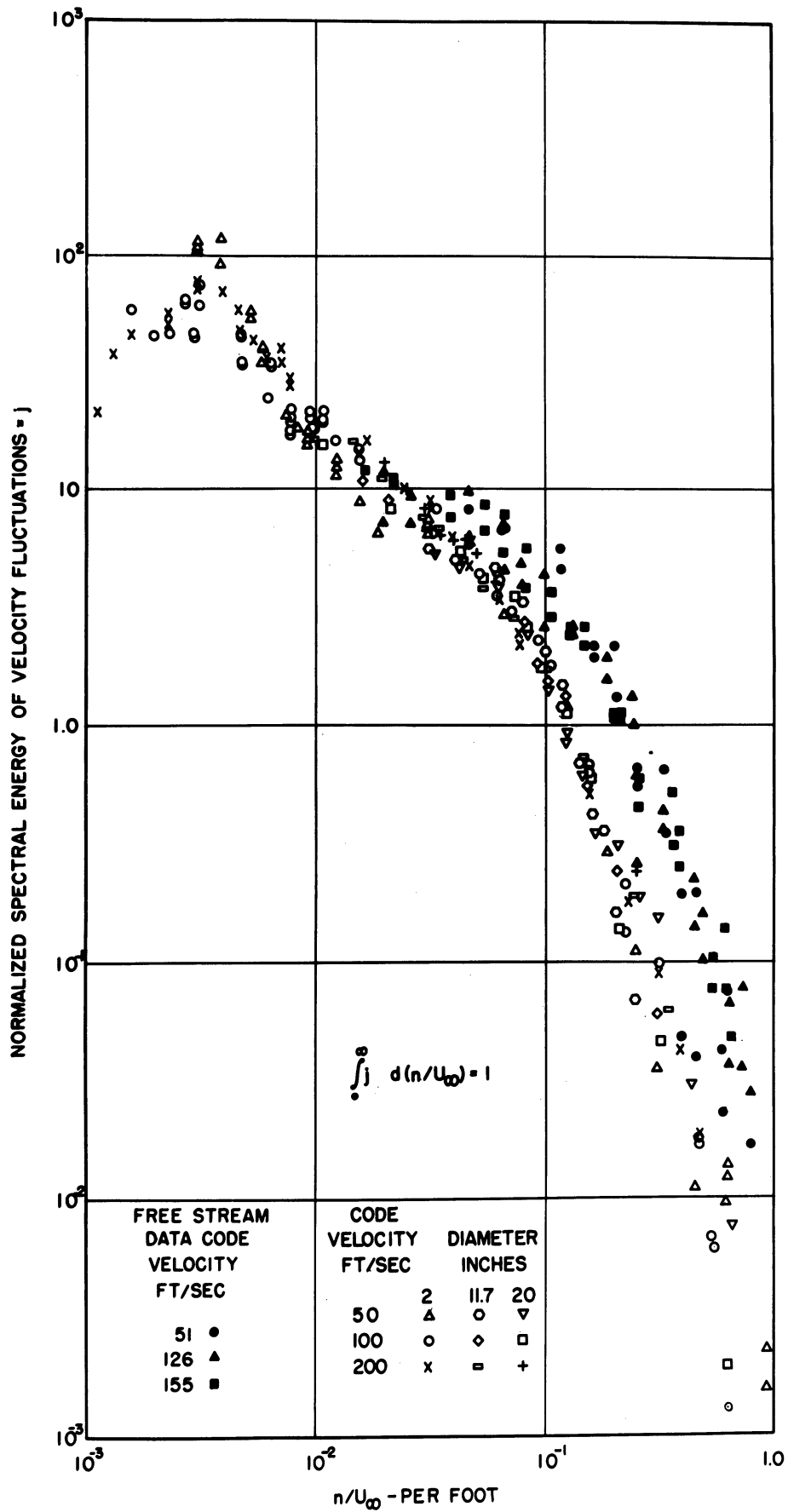


Fig. 7. Normalized spectral energy of velocity fluctuations at  $7^\circ$  from nose.

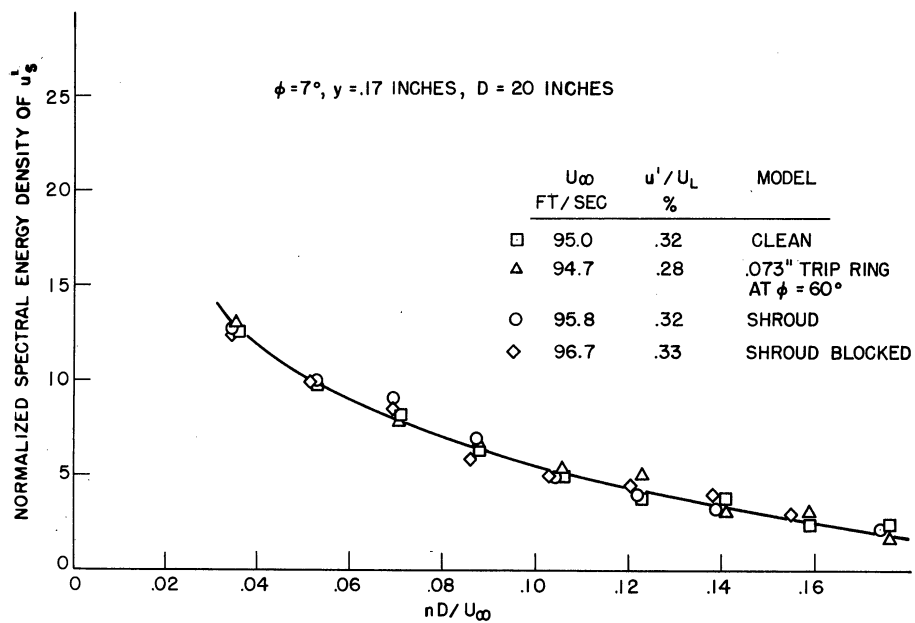


Fig. 8. Normalized spectral energy of velocity fluctuations at  $7^\circ$  from nose on 20 in. diameter body with various flow disturbances.

DISTRIBUTION LIST

(One copy unless otherwise noted)

Commander	10	Commander	
Armed Services Technical		Air Force Special Weapons Center	
Information Agency		Kirtland Air Force Base, New Mexico	
Arlington Hall Station		Attn: SWOI	
Arlington 12, Virginia			
Attn: TIPDR		Commander	
		Air Force Missile Development	
Commander		Center	
Air Force Ballistic Missile Division		Holloman Air Force Base	
Air Force Unit Post Office		Alamogordo, New Mexico	
Los Angeles 45, California		Attn: HDOI	
Attn: WDSOT			
		Commander	
Commander		Air Force Missile Test Center	
Air Force Office of Scientific		Patrick Air Force Base	
Research		Cocoa, Florida	
Tempo X		Attn: MTOI	
Washington 25, D.C.			
Attn: Mechanics Division	2	Commander	
Attn: Library, SRLT	2	Wright Air Development Division	
		Wright-Patterson Air Force Base	
Commander		Ohio	
Air Materiel Command		Attn: Aircraft Laboratory	
Wright-Patterson Air Force Base		Attn: WCOSI	2
Ohio		Attn: WCOSR	2
Attn: Library		Attn: Aeronautical Research Lab.	
		Attn: WCLC	
Commander		Attn: Director, Weapons Systems	
Air Research and Development		Operations	
Command, Attn: Library			
Andrews Air Force Base		Commandant	
Washington 25, D.C.		Air Force Institute of Technology	
		Wright-Patterson Air Force Base	
Commander		Ohio	
Arnold Engineering Development		Attn: MCLI	
Center			
Post Office Box 162		Director	
Tullahoma, Tennessee		Air University Library	
Attn: AEOIM		Maxwell Air Force Base, Alabama	
Commander		Commander	
Air Force Flight Test Center		Air Proving Ground Center	
Edwards Air Force Base		Eglin Air Force Base	
Muroc, California		Florida	
Attn: FTOTL		Attn: ACOT	

DISTRIBUTION LIST (Continued)

Commander  
Air Force Cambridge Research Center  
L. G. Hanscom Field  
Bedford, Massachusetts  
Attn: CROT

P. O. Box AA  
Wright-Patterson Air Force Base  
Ohio

Office of the Chief of Ordnance  
Department of the Army  
Washington 25, D.C.  
Attn: ORDTB

Director  
Ballistics Research Laboratory  
Aberdeen Proving Ground  
Maryland  
Attn: Library

Commanding General  
Office of Ordnance Research  
Department of the Army  
Box CM, Duke Station  
Durham, North Carolina

Commanding General  
Army Rocket and Guided Missile Agency  
Restone Arsenal, Alabama  
Attn: Technical Library, ORDXR-OOL

Commanding General  
White Sands Proving Ground  
New Mexico  
Attn: Technical Library

Chief, Office of Naval Research  
Department of the Navy  
Washington 25, D.C.  
Attn: Mechanics Branch  
Attn: Air Branch

Commanding Officer  
Naval Research Laboratory  
Washington 25, D.C.  
Attn: Documents Library

Chief, Bureau of Aeronautics  
Department of the Navy  
Washington 25, D.C.  
Attn: Research Division

Commander  
U. S. Naval Ordnance Laboratory  
White Oak, Silver Spring, Md.  
Attn: Library (Dr. H. H. Kurzweg)

Superintendent  
Naval Postgraduate School  
Monterey, California

Commanding Officer and Director  
David Taylor Model Basin  
Aerodynamics Laboratory  
Washington 7, D.C.  
Attn: Library

Chief, Bureau of Ordnance  
Department of the Navy  
Washington 25, D.C.  
Attn: Res. & Dev. Division  
Attn: Mr. Jerome Persh, Special  
Projects Office, SP-2722

Director  
National Aeronautics and Space  
Administration  
1520 H Street, N.W.  
Washington 25, D.C.  
Attn: Chief, Document Library

Director  
National Bureau of Standards  
U. S. Department of Commerce  
Washington 25, D.C.  
Attn: Library

Aeronautical Engineering Review  
2 East 64th Street  
New York 21, New York

John Crerar Library  
86 E. Randolph Street  
Chicago 1, Illinois

DISTRIBUTION LIST (Continued)

Director  
Office of Technical Services  
U. S. Department of Commerce  
Washington 25, D.C.  
Attn: Technical Reports Section

Johns Hopkins University  
Applied Physics Laboratory  
8621 Georgia Avenue  
Silver Spring, Maryland  
Attn: Library

National Science Foundation  
1951 Constitution Avenue, N.W.  
Washington 25, D.C.  
Attn: Engineering Sciences Division

Johns Hopkins University  
Department of Aeronautics  
Baltimore 18, Maryland  
Attn: Library (Dr. F. H. Clauser)

U. S. Atomic Energy Commission  
Technical Information Service  
1901 Constitution Avenue, N.W.  
Washington 25, D.C.

University of Maryland  
College Park, Maryland  
Attn: Engineering Library

U. S. Atomic Energy Commission  
Technical Information Extension  
P. O. Box 62  
Oak Ridge, Tennessee

Massachusetts Institute of Technology  
Naval Supersonic Laboratory  
Cambridge 39, Massachusetts

Southwest Research Institute        2  
8500 Culebra Road  
San Antonio 6, Texas  
Attn: Applied Mechanics Reviews

Massachusetts Institute of Technology  
Cambridge 39, Massachusetts  
Attn: Library (Mech. & Aero. Eng.  
and Mechanics)

Georgia Institute of Technology  
Department of Mechanical Engineering  
Atlanta, Georgia  
Attn: Library

Midwest Research Institute  
425 Volker Boulevard  
Kansas City 10, Missouri  
Attn: Library

Harvard University  
Department of Engineering Sciences  
Cambridge 38, Massachusetts  
Attn: Library

University of Minnesota  
Institute of Technology  
Minneapolis, Minnesota  
Attn: Engineering Library

Illinois Institute of Technology  
Armour Research Foundation  
Chicago, Illinois  
Attn: Library

Rosemount Aeronautical Laboratories  
University of Minnesota  
Department of Aeronautical Engineering  
Minneapolis, Minnesota  
Attn: Library

University of Maryland  
Institute for Fluid Dynamics and  
Applied Mathematics  
College Park, Maryland

University of Southern California  
Engineering Center  
3518 University Avenue  
Los Angeles 7, California  
Attn: Library

DISTRIBUTION LIST (Continued)

North Carolina State College  
Division of Engineering Research  
Raleigh, North Carolina  
Attn: Technical Library

Polytechnic Institute of Brooklyn  
Department of Aero. Eng. and  
Applied Mechanics  
333 Jay Street  
Brooklyn 1, New York  
Attn: Library

Aerodynamics Laboratory  
Polytechnic Institute of Brooklyn  
527 Atlantic Avenue  
Freeport, New York

The Pennsylvania State University  
Dept. of Aeronautical Engineering  
University Park, Pennsylvania  
Attn: Library

The James Forrestal Research Center  
Princeton University  
Princeton, New Jersey  
Attn: Library (Prof. S. Bogdonoff)

Rensselaer Polytechnic Institute  
Department of Aeronautical Engineering  
Troy, New York  
Attn: Library

Stanford University  
Department of Aeronautical Engineering  
Stanford, California  
Attn: Library

Defense Research Laboratory  
University of Texas  
Post Office Box 8029  
Austin 12, Texas

University of Washington  
Department of Aeronautical Engineering  
Seattle, Washington  
Attn: Library

University of California  
Engineering Department  
Los Angeles, California  
Attn: Library (Prof. M. K. Boeltes)

Harvard University  
Department of Applied Physics  
Cambridge 38, Massachusetts  
Attn: Library (Prof. H. W. Emmons)

University of Illinois  
Aeronautical Institute  
Urbana, Illinois  
Attn: Library (Prof. H. O. Barthel)

Lehigh University  
Department of Physics  
Bethlehem, Pennsylvania  
Attn: Library (Prof. H. J. Emrich)

Massachusetts Institute of Technology  
Fluid Dynamics Research Group  
Cambridge 39, Massachusetts  
Attn: Dr. L. Trilling

Princeton University  
Dept. of Aeronautical Engineering  
Princeton, New Jersey  
Attn: Library

Stanford Research Institute  
Documents Center  
Menlo Park, California  
Attn: Acquisitions

New York University  
Institute of Mathematical Sciences  
New York 3, New York  
Attn: Library

Aerojet Engineering Corporation  
6352 N. Irwindale Avenue  
Box 296  
Azusa, California  
Attn: Chief,  
Technical Library



DISTRIBUTION LIST (Continued)

Allied Research Associates  
43 Leon Street  
Boston 5, Massachusetts  
Attn: Library (Dr. T. R. Goodman)

AVCO Manufacturing Company  
Research Laboratories  
2385 Revere Beach Parkway  
Everett 49, Massachusetts  
Attn: Chief, Technical Library

AVCO Manufacturing Company  
Research and Advanced Development  
Division  
201 Lowell Street  
Wilmington, Massachusetts  
Attn: Research Library, Mrs. Page

Bell Aircraft Corporation  
P. O. Box 1  
Buffalo 5, New York  
Attn: Library

Boeing Company  
P. O. Box 3107  
Seattle 14, Washington  
Attn: Library

Chance-Vought Aircraft, Inc.  
Dallas, Texas  
Attn: Library

CONVAIR  
Fort Worth Division  
Fort Worth 1, Texas  
Attn: Library

CONVAIR  
P. O. Box 1011  
Pomona, California  
Attn: Library

CONVAIR  
Astronautics Division  
San Diego 12, California  
Attn: Library

CONVAIR  
Scientific Research Laboratory  
P. O. Box 950  
San Diego 12, California  
Attn: Library

CONVAIR  
San Diego Division  
San Diego 12, California  
Attn: Library (Chief, Applied  
Research)

Cornell Aeronautical Labs., Inc.  
4455 Genesee Street  
Buffalo 21, New York  
Attn: Library

Flight Sciences Laboratory  
1965 Sheridan Drive  
Buffalo 23, New York

Douglas Aircraft Company, Inc.  
827 Lapham Street  
El Segundo, California  
Attn: Library

Douglas Aircraft Company, Inc.  
3000 Ocean Park Boulevard  
Santa Monica, California  
Attn: Library

Fairchild Engine and Aircraft Co.  
Guided Missiles Division  
Wyandanch, L. I., New York  
Attn: Library

General Applied Science Labs., Inc.  
Meadowbrook National Bank Bldg.  
60 Hempstead Avenue  
Hempstead, New York

General Electric Company  
Aeroscience Laboratory - MSVD  
3750 D Street  
Philadelphia 24, Pennsylvania  
Attn: Library (Dr. H. Lew)

DISTRIBUTION LIST (Continued)

General Electric Company  
Aircraft Gas Turbine Division  
Cincinnati 15, Ohio  
Attn: Library

General Electric Company  
Research Laboratory  
P. O. Box 1088  
Schenectady 5, New York

General Electric Company  
Special Defense Products Division  
3198 Chestnut Street  
Philadelphia 4, Pennsylvania

Grumman Aircraft Engineering  
Corporation  
Bethpage, L. I., New York  
Attn: Library

Hughes Aircraft Company  
Research and Development Laboratories  
Culver City, California  
Attn: Library

Lockheed Aircraft Corporation  
P. O. Box 551  
Burbank, California  
Attn: Library

Lockheed Aircraft Missile Systems  
Division  
Palo Alto, California  
Attn: Library

Marquardt Aircraft Corporation  
Van Nuys, California  
Attn: Library

The Martin Company  
Baltimore 3, Maryland  
Attn: Library

McDonnell Aircraft Corporation  
P. O. Box 516  
St. Louis 66, Missouri  
Attn: Library

North American Aviation, Inc.  
Missile Division  
12214 Lakewood Boulevard  
Downey, California  
Attn: Library

Northrop Aircraft, Inc.  
Hawthorne, California  
Attn: Library

The Ramo-Woolridge Corporation  
5730 Arbor Vitae  
Los Angeles 45, California  
Attn: Chief Librarian

Rand Corporation  
1700 Main Street  
Santa Monica, California

Republic Aviation Corporation  
Farmingdale, L. I., New York  
Attn: Library

RIAS, Inc.  
7212 Bellona Avenue  
Baltimore 12, Maryland  
Attn: Library

United Aircraft Corporation  
Research Department  
400 Main Street  
East Hartford 8, Connecticut  
Attn: Library

VITRO Laboratories  
West Orange Laboratory  
200 Pleasant Way  
West Orange, New Jersey

Westinghouse Electric Corporation  
Aviation Gas Turbine Division  
P. O. Box 288  
Kansas City, Missouri  
Attn: Engineering Library

DISTRIBUTION LIST (Concluded)

Institute of Aeronautical Sciences  
2 East 64th Street  
New York 21, New York  
Attn: Library

Brown University  
Division of Engineering  
Providence 12, Rhode Island  
Attn: Library

University of California  
Institute of Engineering Research  
Low Pressures Research Project  
Berkeley 4, California

Jet Propulsion Laboratory  
California Institute of Technology  
4800 Oak Grove Drive  
Pasadena 3, California  
Attn: Library (Dr. P. Wegener)

Guggenheim Aeronautical Laboratory  
California Institute of Technology  
Pasadena 4, California  
Attn: Aeronautics Library  
(Prof. H. W. Liepmann)

Carnegie Institute of Technology  
Pittsburgh 18, Pennsylvania  
Attn: Library

Catholic University of America  
Aeronautical Mechanical Engineering  
Washington 17, D.C.  
Attn: Library

Cornell University  
Graduate School of Aeronautical  
Engineering  
Ithaca, New York  
Attn: Library (Dr. W. R. Sears)

Columbia University  
Department of Civil Engineering &  
Engineering Mechanics  
New York 27, New York  
Attn: Library (Prof. G. Herrmann)

University of Florida  
Engineering Mechanics Department  
Gainesville, Florida  
Attn: Library

Director  
Aeronautical Research Institute  
University of Tokyo  
Komaba, Meguro-Ku  
Tokyo-Japan

Director  
National Aeronautical Establishment  
Ottawa, Ontario, Canada

Training Center for Experimental  
Aerodynamics  
Rhode-Saint-Genese (Belgique)  
72, Chaussee de Waterloo  
Belgium  
Attn: Library

Chairman  
Defence Research Board  
Ottawa, Ontario, Canada  
Attn: DSIS

University of Witwatersrand  
Milner Park  
Johannesburg  
Union of South Africa  
Attn: Library

University of Toronto  
Institute of Aerophysics  
Toronto 5, Canada  
Attn: Library

Commander, European Office 2  
Air Research and Development Command  
Shell Building  
47 Rue Cantersteen  
Brussels, Belgium





